Effect of Accelerated Ultraviolet (UV) Weathering on Firefighter Protective Clothing Outer Shell Fabrics

Rick Davis
Materials Flammability Group
Fire Research Division
Building and Fire Research Laboratory

Joannie Chin, Chiao-Chi Lin, and Sylvain Petit
Polymeric Materials Group
Materials and Construction Research Division
Building and Fire Research Laboratory

ABSTRACT

The Outer Shell of the jacket and pants of the firefighter's protective clothing is constructed of a fabric that is commonly a blend of polyaramid, polybenzimidazole, and/or poly(melamine-formaldehyde) fibers. The Outer Shell contributes to the thermal and moisture protection of the garment, but its primary purpose is to provide protection from other physical hazards, such as sharps objects and abrasive surfaces. The research discussed in this manuscript indicates the mechanical performance, which is critical to the Outer Shell providing protection against these physical hazards, of polyaramid and polybenzimidazole based Outer Shells will rapidly deteriorate when exposed to ultraviolet light at 50 °C and 50% relative humidity. For example, as high as an 80% reduction in the tear and tensile strength was measured after 13 d of exposure to these conditions. The mechanical performance deterioration resulted from photo-induced decomposition of the polymer backbone, as measured by infrared spectroscopy. Polymer and fiber decomposition was also visually observed using confocal microscopy. These microscopy images showed the exposure conditions caused pitting on the surface of the fibers, fiber shape deformation, and/or a switch from ductile to brittle failure. Even though the exposure conditions caused catastrophic mechanical failure, the amount of ultraviolet light transmitted through these fabrics is insufficient to photolytic degrade the undergarments of the protective clothing.

Key Words: Firefighter protective clothing, turnout gear, polyaramid, polybenzimidazole, polymer fiber, NIST SPHERE, tear strength, tensile strength, laser scanning confocal microscopy, ultraviolet transmittance, fourier transform infrared (FTIR) spectroscopy, textiles, service life, polymer aging.

Introduction

Structural firefighter protective clothing, such as jacket, boots, and helmet, is designed to shield the firefighter from environmental hazards, such as heat and chemical exposures, and abrasive surfaces. The turnout gear (jacket and pants only) is typically a three layer system consisting of an Outer Shell (OS), Moisture Barrier (MB), and Thermal Liner (TL), as shown in Figure 1[1]. The inner-most layer is the Thermal Liner, which primarily provides thermal protection. This layer consists of a facecloth, which slides easily along the skin to reduce the work required to move, and a spun-laced nonwoven insulating fabric. The air in the woven fabric provides the thermal protection; therefore, the thicker the nonwoven fabric the better the thermal protection. However, a thicker TL is heavier and less breathable, and thus less comfortable.

The middle layer is the Moisture Barrier (MB). It is primarily a poly(tetrafluoroethylene) permeable film barrier laminated to a thin polyaramid woven or nonwoven backing substrate. The membrane prevents the transport of chemicals, pathogens, and water from the environment to the firefighter. The transport of any liquids across the MB toward the firefighter is a severe concern as it adds significant mass to the garment and deteriorates the TL performance, both of which can lead to death from thermal exposure and heat stress. The backing substrate increases the durability of the TL. The nonwoven backing is less durable than the woven, but provides additional thermal protection.

The OS is the outermost layer and is the first and only line of defense against the abrasive and sharp physical hazards common to a fire scene. However, the OS also provides 25% to 30% of the turnout gear's thermal protection and serves to reduce water absorption (until the water-repellant finish is removed by dirt, abrasion, or laundering). The OS is a woven fabric with a rip-stop construction being preferred as it prevents tear propagation. Similar to the TL, the OS is commonly constructed of polyaramid, polybenzimidazole, and/or poly(melamine-formaldehyde) fibers.

Researchers have published the impacts of simulated environmental conditions on fibers that are similar to those used in firefighter turnout gear. Zhang et al [2] has shown the mechanical properties (tenacity, modulus, break extension and energy at break) for poly(*p*-phenylene terephthalamide) type fibers deteriorated linearly over 145 h of continuous ultraviolet exposure. The carbon arc lamp used in this study provided non-uniform light intensity across a portion of the UV spectrum (350 cm^{-1} to 420 cm^{-1} with intensity maximums at 360 cm^{-1}, 380 cm^{-1}, and 390 cm^{-1}). The exposure conditions were maintained at 40 °C ± 3 °C and 45% relative humidity (RH). Chin et al [3] has shown that poly(p-phenylene-2,6-benzobisoxazole) fibers lost 30% tensile strength after a sequential exposure of 50 °C/60% RH (84 d) and 60 °C/37% RH (73 d). UV exposure was not investigated. Walter et al [4] has shown the mechanical properties (percent elongation and tenacity) of poly(*m*-phenylene isophthalate) type fibers deteriorated over

120 h of continuous exposure to a carbon lamp UV source and environmental conditions of 65 °C and 40% RH.

The study presented in this manuscript is focused on commercially available Outer Shell fabrics. These woven fabrics were exposed to ultraviolet (UV) radiation (295 cm^{-1} to 495 cm^{-1}) at conditions similar to what is expected for firefighter protective clothing that is in-service (50 °C and 50% RH), and for a sufficient exposure duration to understand the impact these conditions will have over the typical service life (10 y) of turnout gear. The performance of new fire fighting protective clothing and the guidelines for selecting, caring, and maintaining in-service protective clothing is defined in the United States by the National Fire Protection Association[5 , 6]. Recent amendments to these documents have indicated that ultraviolet exposure can damage the turnout gear; therefore, "do not store your gear in direct sunlight." The goal of this research was to determine the impact of UV exposure (under typical in-service conditions) on fabrics commonly used in Outer Shells of commercial turnout gear and to determine to what extent the undergarments could be damaged from UV transmission through the OS.

Experimental*

Description of Fabrics

Kombat™ and Defender™ 750 are commercially available Outer Shells commonly used in firefighter turnout ensembles.[7] Kombat™ is a 40%/60% rip-stop weave fabric of polybenzimidazole and poly(*p*-phenylene terephthalamide) with a water repellant coating called Super Shelltite™ [8]. Defender™ is a 93%/5%/2% plain weave fabric of poly(*m*-phenylene isophthalate), poly(*p*-phenylene terephthalamide), and P-140 (antistatic fiber). This product has a water repellant coating called Shelltite™ [8]. These polymers are more commonly known as PBI® (polybenzimidazole)[9], Kevlar® (poly(*p*-phenylene terephthalamide))[10], and Nomex® (poly(*m*-phenylene isophthalate))[10]. Please refer to Table 1 for more information about these fabrics, Figure 2 for pictures of these fabrics, and Figure 3 for the chemical structure of the polymers. For the remainder of this report these fabrics will be referred to NKB (Defender™ 750) and PKB (Kombat™).

Fabrics were delivered on standard fabric rolls and stored as-received at ambient conditions (25 °C, ± 5 °C and 20% ± 5% relative humidity) in closed containers. The containers were not completely sealed, which allowed the fabrics to be conditioned to the room conditions over the 10 months before testing. The room was kept dark when not in use; therefore, during storage and testing, the fabrics were exposed to very little of the low ultraviolet fluorescent lights in the storage room.

* Certain commercial equipment, instruments or materials are identified in this paper in order to specify the experimental procedure adequately. Such identification is not intended to imply recommendation or endorsement by the National Institute of Standards and Technology, nor is it intended to imply that the materials or equipment identified are necessarily the best available for this purpose.

The fabrics were cut into 10.2 cm by 7.6 cm (4 in x 3 in) swatches for the UV exposure conditioning, measuring ultraviolet (UV) radiation transmission, and to confirm chemical structure by attenuated total reflectance-Fourier transform infrared spectroscopy (FTIR). From these swatches was cut 6.8 cm x 2.5 cm (2.66 in x 1.0 in) specimens for measuring tear strength (Figure 4). Following the tear strength experiments, the tensile strength was measured on the ply-twisted yarns from the non-torn, long edge of these tear strength specimens. After both mechanical performance experiments were complete, the surface morphology and fracture ends of the ply-twisted yarns were studied using laser scanning confocal microscope. This same workflow was used for both the unexposed and the UV exposed fabrics.

UV Aging

Accelerated UV aging of the fabrics was performed using the NIST SPHERE (Simulated Photodegradation via High Energy Radiant Exposure). High UV irradiance accelerated exposures were carried out in the NIST 2 m integrating sphere-based weathering device, referred to as SPHERE (Simulated Photodegradation *via* High Energy Radiant Exposure). The mercury arc lamp system used with SPHERE produces a collimated and highly uniform UV flux at each of the 32 testing ports (environmental chambers). A borosilicate glass window between the lamp system and the integrating sphere eliminated all UV wavelengths < 290 nm and a dichroic reflector in the lamps removed wavelengths > 450 nm. Additional details on the construction and properties of the SPHERE have been published elsewhere.[11]

The fabric exposure environment in the SPHERE environmental chambers was precisely controlled at 50 °C ± 0.1 °C and 50% ± 1% relative humidity (RH). Periodically specimens were removed to perform the workflow analysis and tests discussed above.

The NIST SPHERE exposes specimens to the above-described conditions for the entire 24 h of a day. The calculated daily UV exposure dosage for these fabrics is 15.9 kJ/m^2 ± 0.02 kJ/m^2. Based on this daily dosage and the calculation of a representative daily natural dose (using data from the terrestrial tables in ASTM G159), 1 d on the SPHERE is equivalent to 7.4 d of continuous sun. Assuming in a day of natural exposure there is 9 hours of sun and 15 hours of darkness then 1 d on the SPEHRE is equivalent to 19.7 d of natural exposure.

Material Characterization

Tear Strength: Tear strength experiments and data analysis were performed as described in ASTM D 2261-96.[12] The experiments were conducted on an Instron model 5582 universal testing machine (Instron Corporation) equipped with custom grips as shown in Figure 5(a**).** The tear strength specimens were 6.8 cm x 2.5 cm (2.66 in x 1.0 in) with a single 2.5 cm (1.0 inch) tear introduced at one end as shown in Figure 4(a). All testing was carried out in the same fabric direction; i.e., either warp or fill direction. Although it was difficult to determine which direction

(warp or fill) the specimens were extracted from, care was taken to ensure that all of the specimens were consistently extracted from the same fabric direction. The gauge length between grips was 2.5 cm, and crosshead speed was 50 mm/sec. Four replicates of each fabric were tested per sampling interval.

Yarn Tensile Strength and % Elongation (at Break): A TA Instruments RSA III Dynamic Mechanical-Thermal Analyzer (DMTA) (TA Instruments-Waters LLC, New Castle, DE) with transient capability was used to obtain the load-extension properties of ply-twisted yarn extracted from the non-torn side of the tear testing specimens. As shown in Figure 5(b), testing was carried out using fiber and film grips provided by the manufacturer. Specimen gauge length was 10 mm and specimen extension rate was 0.005 mm/sec. A preload of 0.02 N ± 0.01 N was introduced to reduce slack in the ply-twisted yarn when it was secured on the fiber and film grips. A minimum of ten individual ply-twisted yarns were analyzed per sampling interval.

During the early methods development stage of this study, tensile strength of fabric strips was performed as described in ASTM D 5035-36. While the absolute values differed the trends were directly aligned with results obtained on yarn using the DMTA. Due to material limitations, we elected to use the DMTA and yarn for measuring the tensile strength for the remainder of the study.

Laser Scanning Confocal Microscopy: Zeiss Model LSM510 and LSM510 META (*Carl Zeiss, Inc.*, Oberkochen, Germany) reflection Laser Scanning Confocal Microscopes (LSCM) with the same objectives were employed to qualitatively characterize the fiber surface and fracture end morphology of NKB and PKB. The incident laser wavelength was 543 nm for both of the two LSCMs. By adjusting the focal plane in the z-direction, a series of single images (optical slices) were stacked and digitally summed over the z-direction to obtain a 3-D image. The *z*-direction step size was 0.1 μm using objectives of 20x, 50x, and 150x. The pixel size of the LSCM images is 512 pixels by 512 pixels. At least two observations on three or more fiber samples were carried out per sampling interval.

Ultraviolet Transmittance: Figure 6 shows the schematics of the UV transmittance measurement. The UV source was provided by the NIST SPHERE with the output intensity of 480 W/m^2 [**Error! Bookmark not defined.**]. UV-visible transmittance was measured using a Hewlett Packard 8452A diode array UV-Vis spectrophotometer (HP, Agilent) with a custom integrating sphere collector. UV spectra were recorded between 290 nm to 690 nm before (to record the dark current) and after the fabric specimen was mounted on black felt. At least three measurements were taken per sampling interval. The distance between the integrating sphere and the fabric specimen was a constant 2 cm for each measurement. Due to dark current drift, the calculated UV protection factor (UPF) and the average UV transmittance may be slightly shifted from the exact values.

Attenuated Total Reflectance Fourier Transform Infrared (ATR-FTIR) Spectroscopy: Infrared analysis was carried out using a Nicolet Nexus 670 FTIR (Nicolet Instrument Corporation) equipped with a mercury cadmium telluride (MCT) detector and a SensIR Durascope (Smiths Detection) attenuated total reflectance (ATR) accessory. Consistent pressure on the yarns was applied using the force monitor on the Durascope. Dry breathing quality air was used as the purge gas. FTIR spectra were recorded at nine different locations on each 10.2 cm x 7.6 cm (4 in x 3 in) fabric swatch and were averaged over 128 scans. Spectral analysis, including spectral baseline correction and normalizing, was carried out using a custom software program developed in the Polymeric Materials Group at NIST to catalogue and analyze multiple spectra.[13] The spectra were baseline corrected and normalized using the peak at 781 cm^{-1} for NKB, and the peak at 820 cm^{-1} for PKB, both of which are attributed to out-of-plane aromatic C-H bending. Standard uncertainties associated with this measurement are ± 1 cm^{-1} in wavenumber and ± 5 % in absorbance.

Results and Discussion

Tear and Tensile Strength

Figure 7 is a representative load-extension curve obtained from the tear strength testing of (a) NKB and (b) PKB fabrics. As described in ASTM D2261-96[12], the average of the five highest load points is used to calculate the tear strength values, which are shown in Figure 8 and Tables 2 and 3. NKB was exposed and analyzed first with the PKB studies following immediate afterwards. Based on the data collected from NKB, we reduced the exposure time and the testing frequency for PKB, which is the reason the exposure days in Table 2 are not exactly aligned with those in Table 3. The calculated natural exposure days is based on 1 d on the SPEHRE being equivalent to 7.4 days of natural exposure as discussed in the Experimental section of this document.

For NKB, the largest deterioration of tear strength loss occured after 1 d of exposure (a 43% decrease to a value of 43.18 N ± 5.13 N) (Table 2). After another 2.6 d of exposure, the tear strength dropped a total of 73% to a value of 20.04 N ± 1.08 N. The performance deterioration slowed down over the next 15.5 d with only an average drop of 6.5% between (3.6 and 7) d, (7 and 13) d, and (13 and 29) d. By the time the deterioration reached a steady state at 29 d, the fabric had lost 93% of its original tear strength (to a value of 5.93 N ± 0.65 N) and lost only another 1% of its tear strength over the next 37 d of UV exposure at 50 °C and 50% RH.

Within the experimental error, the tear strength of new PKB (80.56 N ± 4.30 N) is comparable to NKB (75.43 N ± 8.01 N). Similar to NKB, the tear strength of PKB deteriorated rapidly with a 54% decrease (to a value of 37.39 N ± 2.58 N) in 6 d after which the deterioration slowed down with a 16% drop between (6 and 14) d, and another 10% drop between (14 and 28) d. Unlike NKB, the PKB tear strength deterioration did not reach a steady state, but rather continued to

lose another 7% over the last 18 d of the study.

At the same point in the exposure period, the PKB has a tear strength that is on average 180% higher than the NKB, which is especially interesting because the tear strength of the new fabrics is comparable. This data suggests that PKB has superior resistance to these exposure conditions; i.e., the tear strength at 56.6 d for PKB (10.19 N ± 0.20 N) is similar to the tear strength of NKB at 13 d (10.01 N ± 0.26 N).

Representative strain-strain curves for the yarn tensile strength experiments conducted on the DMTA using the UV exposed and unexposed NKB and PKB abrics are shown in Figure 9. In calculating the stress, it was assumed that the cross section of ply-twisted yarn is circular and the geometry is cylindrical. Though the tensile strength of the yarn was not the same as the tensile strength measured on pieces of fabric, previous internal experiments determined the trends were aligned. The 0.02 N ± 0.01 N preload did not completely remove the slack as evidenced by the delayed increase in load until an approximate extension of 1.2 mm and 0.25 mm for NKB and PKB, respectively. The slack has been corrected for the stress-strain data in Figure 10 and Tables 4 and 5 by linearly fitting the linear-elastic region and shifting the curve to zero extension.

The unexposed NBK has a well defined yield point, a 55.2 MPa ± 7.97 MPa tensile strength, and 40.89% ± 4.07% elongation (Figure 10 and Table 4). Similar to the deterioration in tear strength, the tensile strength and percent elongation also deteriorated rapidly with a 40% and 55% decrease in the tensile strength and percent elongation, respectively, after 1 d of UV exposure at 50 °C and 50% RH. The tensile strength continued to follow a very similar deterioration profile as discussed above for the tear strength with another drastic drop in performance (28% decrease to a value of 17.56 MPa ± 2.09 MPa) over the next 2.6 d, which is followed by a slower performance deterioration over the next 24.4 d (26% decrease to a value of 3.18 MPa ± 0.92 MPa) and reaching a steady state for the reminder of the exposure time with a final tensile strength of 1.31 MPa ± 0.27 MPa (98% total decrease). The decrease in percent elongation is more severe than the tear and tensile strength as it decreased an additional 35% between (0.9 and 3.6) d, then reached a steady state for the remainder of the exposure time with a final percent elongation of 6.19% ± 1.81% (85% decrease).

The tensile strength performance for NBK and PKB is very similar to the measured tear strength deterioration discussed above. The PKB has superior resistance to the exposure conditions as evidenced by PKB having a less severe tensile strength deterioration rate and higher tensile strength over the course of exposure (Figure 10 and Tables 4 and 5). More specifically, the tensile strength for unexposed NKB (55.2 MPa ± 7.97 MPa) and unexposed PKB (55.03 MPa ± 5.30 MPa) are the same within the uncertainty of the measurement. However, a tensile strength of 10.56 MPa ± 0.88 MPa was measured at 7 d for NKB, but a value of 10 MPa is calculated not to occur until 50 d for PKB.

A similar trend in percent elongation deterioration was also measured (Figure 10 and Tables 4 and 5), where the PKB has a less severe deterioration rate. While the percent elongation for the unexposed PKB (4.17% ± 0.29%) is an order of magnitude lower than the unexposed NKB (40.90% ± 4.07%), the percent elongation for these two fabrics are significantly closer after 7 d of exposure with values in the range of 2.69% to 6.16%.

UV Transmittance

The use of factors, such as the UV protection factor (UPF) and the average UV transmittance, aids in quantifying the UV protection properties of garments [14,15,16], such as the Outer Shell of firefighter protective clothing. As the transmission of UV light through the OS increases (UPF decreases) there is an increasing potential for UV radiation damage to the underlying layers (moisture barrier and thermal liner) of the protective gear and/or the firefighter's skin.

According to AATCC test method 183-2000 [14], UPF is calculated by

$$\mathrm{UPF} = \frac{\sum_{280nm}^{400nm} E_\lambda \times S_\lambda \times \Delta\lambda}{\sum_{280nm}^{400nm} E_\lambda \times S_\lambda \times T_\lambda \times \Delta\lambda} \tag{1}$$

where E_λ is relative erythemal effectiveness function, S_λ is solar spectral irradiance (W/cm^2/nm), T_λ is the measured spectral transmittance of the fabric (%), $\Delta\lambda$ is the measured wavelength interval (nm). The average A-range ultraviolet transmittance was calculated by

$$T_{(UV-A)}^{av} = \frac{\sum_{315nm}^{400nm} T_\lambda \times \Delta\lambda}{\sum_{315nm}^{400nm} \Delta\lambda} \tag{2}$$

and the average B-range ultraviolet transmittance was calculated by

$$T_{(UV-B)}^{av} = \frac{\sum_{280nm}^{315nm} T_\lambda \times \Delta\lambda}{\sum_{280nm}^{315nm} \Delta\lambda} \tag{3}$$

Both the unexposed NKB and PKB provide outstanding UPF protection (Tables 6 and 7).[16,17] After 13 d of UV exposure at 50 °C and 50% RH, the UPF deteriorates by 53% to 23.9 for the NKB, which is the same UPF value for the unexposed PKB. A 4% decrease over the next 16 d of exposure for NKB is followed by a steady state UPF value of 17.93 ± 0.3 for the remaining 27 d of exposure. The PKB UPF deterioration is similar to NKB from 13 d through the end of the exposure. These results indicate no significant deterioration of UV blocking performance of either fabric has occurred even though the mechanical properties have significantly deteriorated. The excellent UV blocking performance of these fabrics is likely maintained due to the high fiber density. These results indicate the undergarments will not be exposed to sufficient UV radiation through the OS for this pathway to be a concern for UV-induced deterioration of the TL or MB.

Laser Scanning Confocal Microscopy

LSCM was used to visually observe the fiber morphology and fracture ends (Figures 11 to 16). LSCM images of the poly(*m*-phenylene isophthalate) fibers from NKB are shown in Figures 11 and 12. LSCM images of PKB are shown in Figures 13 to 16, where Figures 13 and 14 are the poly(*p*-phenylene terephthalamide) brown fibers and Figures 15 and 16 are the polybenzimidazole yellow fibers. While color was the primary mechanism for delineating the poly(*p*-phenylene terephthalamide) brown from the polybenzimidazole yellow fibers, FTIR spectroscopy was frequently used for confirmation.

The poly(*m*-phenylene isophthalate) fibers from NKB were visually inspected under the LSCM at (0, 13, and 66) d of SPEHRE exposure before and following tensile testing (Figures 11 and 12, respectively). After 13 d of UV exposure at 50 °C and 50% RH, the surface of the fiber is rough with an estimated 10% surface pitting. At 66 d, there is an estimated 25% surface pitting and the surface is significantly rougher with a multitude of intersecting surface channels. These observations are classical identifiers of material chemical and/or property decomposition.[18]

Material chemical and property decomposition initiated by UV exposure was further supported by the LSCM images of the fracture ends and surface of the poly(*m*-phenylene isophthalate) fiber following the tensile experiments. The unexposed poly(*m*-phenylene isophthalate) fiber maintains its cylindrical shape and a regular patterned finish (possible surface delamination) is observed that is frequently associated with ductile failure at break (Figure 12a).[18] The "necking" at the fracture end is another indicator of ductile failure of this unexposed fiber. At 13 d of exposure, the failure mechanism has switched from ductile to brittle failure as evidenced by the sharp cleavage and granulated fracture end of the fiber (Figure 12b). In addition to the rough and pitted surface, there is no regular patterned finish and the fiber is slightly deformed. At 66 d, the shape deformation is significant as the fiber appears to be squished into a more oval shaped cylinder. These observations from the LCSM images are consistent with the measured mechanical property deterioration of the NKB fabric.

The poly(*p*-phenylene terephthalamide) fibers from PKB were visually inspected under the LSCM at (0, 14, and 56.6) d of SPEHRE exposure before and following tensile testing (Figures 13 and 14, respectively). The UV exposure had a similar impact on the poly(*p*-phenylene terephthalamide) fibers as just discussed for the poly(*m*-phenylene isophthalate) fibers, except the surface deterioration is significantly more severe in the poly(*p*-phenylene terephthalamide) fibers, 60% surface pitting at 66 days exposure. However, these fibers still maintain a level of ductility as evidenced by the splitting and fibrillation at the fracture ends, but deterioration is still occurring as the ends are becoming more granular with increasing exposure time. Similar to poly(*m*-phenylene isophthalate) fibers, these exposed poly(*p*-phenylene terephthalamide) fibers are also deformed.

The polybenzimidazole fibers from PKB were visually inspected under the LSCM at (0, 14, and 56.6) d of exposure before and following tensile testing (Figures 15 and 16, respectively). The UV exposure had a similar impact on the polybenzimidazole fibers as discussed for the poly(*m*-phenylene isophthalate) fibers, except the fracture end morphology (sharp cleavage) is independent of exposure duration and the surface pitting was less severe (12% at 55.6 d).

Attenuated Total Reflectance Fourier Transform Infrared (ATR-FTIR) Spectroscopy

ATR-FTIR analysis is used to elucidate the chemical changes induced by the UV exposure conditions. The IR peak assignments for the as (a) collected and (b) and difference spectra for NKB (Figure 17) and PKB (Figure 18) are based primarily on literature references.[19,20,21,22,23,24] The difference spectra was generated by subtracting the spectra of the exposed from the spectra of the unexposed fabric. Negative peak (downward-pointing) in the difference spectra are species that are lower in concentration relative to the reference spectrum (unexposed fabric) and positive peaks (upward-pointing) are species that are new or are higher in concentration relative to the reference material.

The key IR peaks for NKB are the Amide I band at 1640 cm^{-1}, Amide II band at 1523 cm^{-1}, and N-H stretching band at 3280 cm^{-1} (Figure 17).[19] After exposure, new (positive) peaks appear for carbonyl stretching (1720 cm^{-1}), C-O stretching (1180 cm^{-1}), and carboxylic acid O-H (3280 cm^{-1}). This observation, along with the reduction in the Amide II peak intensity (negative 1534 cm^{-1} peak), indicates a cleavage of the amide bonds (C-N) in the polymer backbone and the formation of carboxylic acids as well as other oxidized species, presumably by photo-oxidation. The decreasing intensity of the peaks at 2880 cm^{-1} and 2930 cm^{-1} are likely due to a coating applied to the fabric to improve the water repellant performance of the gear, such as Shellite™ [8]. This assumption is primarily based on the polymeric fibers having only sp^2 C-H bonding, while these peaks correspond to sp^3 C-H bonding, which is present in these water repellant coatings. Based on the ATR-FTIR results, UV exposure at 50 °C and 50% RH is causing decomposition of NKB and the water repellant coating.

The key IR peaks for PKB (Figure 18) are the C=C/C=N stretching band of polybenzimidazole at 1620 cm^{-1} as well as peaks for poly(*p*-phenylene terephthalamide), which are similar to those described for above for poly(*m*-phenylene isophthalate) of NKB (Figure 17).[19] After exposure, new peaks appear at 1660 cm^{-1}, 1405 cm^{-1}, and 1076 cm^{-1}, which correspond to carbonyl stretching and C-O stretching from oxidized species and are indicative of photo-oxidation. These peaks, and therefore these species, increase with increasing exposure duration. There is also an increase in the O-H stretching peak center around 3100 cm^{-1}, which suggests the new 1660 cm^{-1} peak corresponds to carboxylic acid, similar to what was observed in NKB. There is also a decomposition of the water-repellant coating as evidenced by the decrease in the 2880 cm^{-1} and 2930 cm^{-1} peaks, which again is consistent with the IR analysis of exposed NKB.

Impact of Exposure on Outer Shell Fabrics

1 d on the SPEHRE is equivalent to 19.7 d of natural light exposure (Tables 2 to 5). By 13 d on the SPHERE the mechanical property deterioration has reached a steady to semi-steady state so all future experiments will be performed only to 13 d, which is the equivalent of 257 d of natural light exposure. Assuming everyday a firefighter is exposing his/her turnout gear to these conditions for 1 h/day, than exposing these fabrics to 13 d on the SPHERE would be equivalent to what a turnout gear would be exposed to in 6.3 years of natural exposure. Therefore, within 6.3 years of natural exposure, the turnout gear with NKB based OS will have lost 83% of its tear strength and 89% of its tensile strength. The PKB based OS will have fared significantly better during this period with only a deterioration of 70% and 51% for the tear and tensile strength, respectively. The LSCM and the ATR-FTIR results suggest these material performance differences are related to chemical decomposition. Since the fabric construction also impacts its mechanical performance, we cannot delineate the chemical decomposition from the fabric construction (plain versus rip-stop) contribution to the performance deterioration.

The UV transmission through these fabrics was the only property not significantly impacted by the exposure conditions. The UPF value decreased by 50% within 13 d of exposure, but the fabrics still blocked 96% of the UV light and 94.5% of the UV light after 56 d of exposure. These results indicate that it is highly unlikely that the undergarments (Moisture Barrier and Thermal Liner) of the turnout gear are exposed to sufficient UV light through the OS for this pathway to be a concern for UV-induced degradation.

Conclusions

The goal of this research was to determine the impact of UV exposure (under typical in-service conditions) on fabrics commonly used in OS of commercial turnout gear and determine to what extent the undergarment could be damaged from UV transmission through the OS. The unexposed PKB and NKB fabrics had similar tear and tensile strength performance and both experienced catastrophic mechanical property deterioration within 1 d of UV exposure at 50 °C and 50% RH. The PKB mechanical property deterioration was significantly less severe having

180% better tear strength and 350% better tensile strength (values are an average across all exposure intervals), as compared to NKB. The chemical composition analysis by ATR-FTIR indicated these exposure conditions had induced polymer decomposition. The LSCM images suggested polymer decomposition has occurred as evidenced by the surface pitting and fiber shape deformation. Brittle failure was also observed for the exposed poly(*m*-phenylene isophthalate) fibers of NKB, but not for the poly(*p*-phenylene terephthalamide) fibers of PKB. The LSCM and ATR-FTIR results were consistent with polymer decomposition, which directly corresponded with the measured deterioration of PKB and NKB mechanical properties. Even though the mechanical properties had significantly deteriorated and the fibers had partially decomposed, the UV transmission through these garments never dropped below 94.5% blockage of UV light. This suggests UV-induced degradation of the undergarments most likely results from another exposure mechanism, such as, the turnout gear is turned inside-out to dry or the OS is separated from the undergarments.

Future Research

There are a number of parameters currently under investigation or planned for in the near future. These include, but are not limited to, measuring the individual contribution of each environmental stress, such as lower temperature and no UV light, measuring the impact these conditions have on other fabric compositions, measuring the thermal performance as a function of these conditions, and evaluating new technologies to mitigate the performance deterioration.

Acknowledgements

Appreciation is extended to Prof. S Lee at National Tsing Hua University in Taiwan for his discussion and guidance throughout this work and Debbie Stanley of NIST for her assistance on UV-transmittance measurements and specimen exposure in the NIST SPHERE.

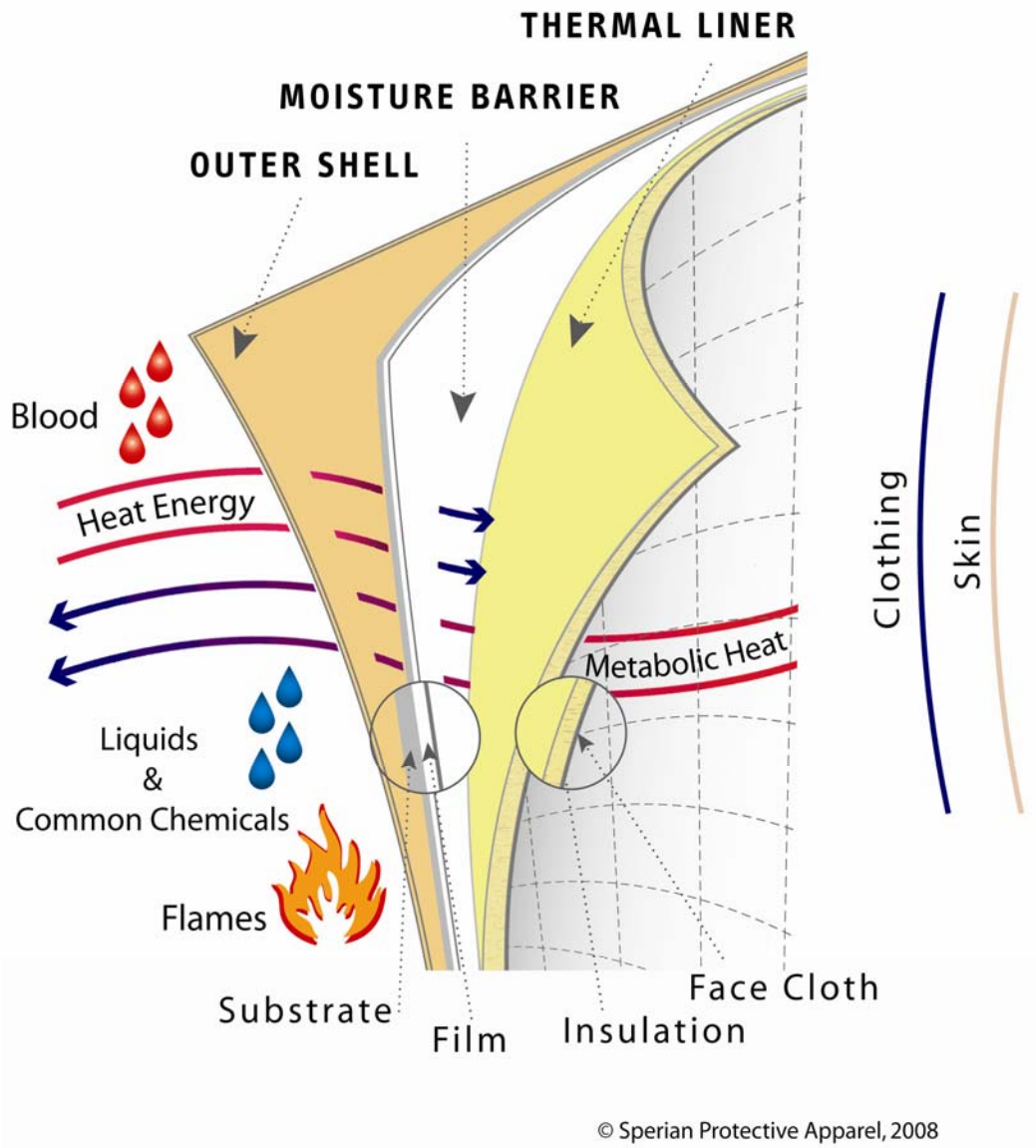

Figure 1. Turnout gear schematic

Table 1. Composition of the fabrics used in this study.

Name	Tradenames	Nomex® (%)	Kevlar® (%)	PBI (%)	P140 (%)	Weight* g/m^2 (oz/yd^2)	Fabric weave type	Water Repellant Finish
NKB	Defender™ 750	93	5	-	2	254 (7.5)	Plain	Shelltite™
PKB	Kombat™	-	60	40	-	254 (7.5)	Rip Stop	Super Shelltite™

*Manufacturer specification called "weight" is the mass per unit area of fabric without accounting for fabric thickness.

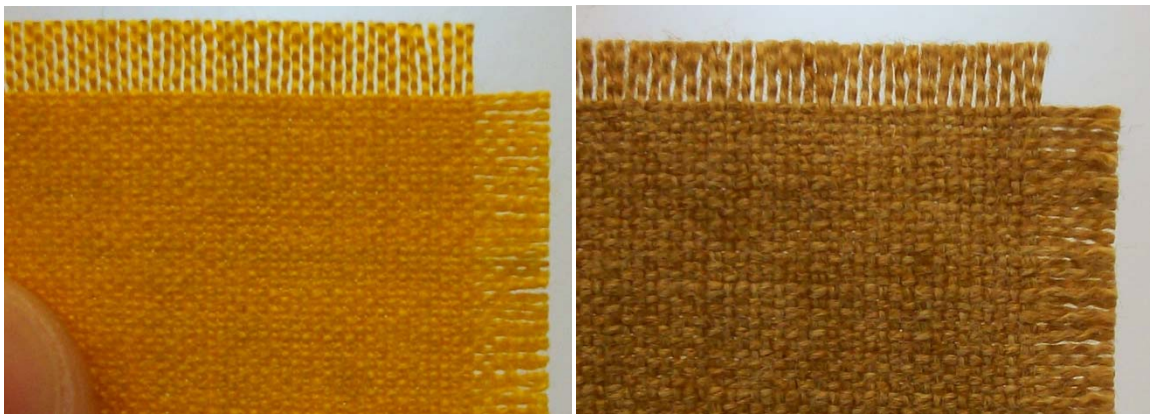

(a) (b)

Figure 2. Photographs of the (a) yellow NKB and the (b) gold/natural PKB fabrics. Note the different weave types and ply-twisted yarn density in the fill and warp direction.

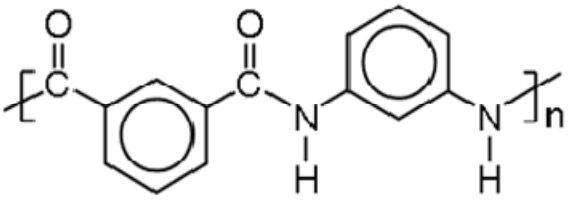

(a)

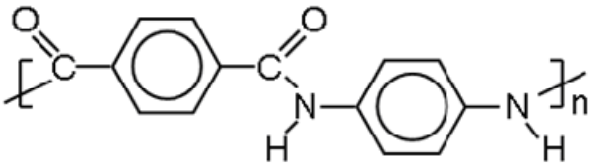

(b)

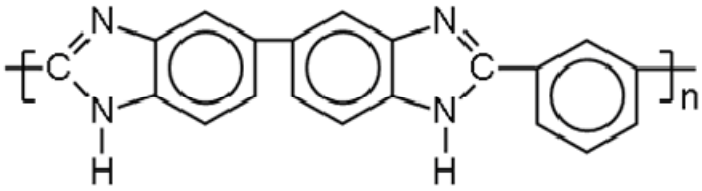

(c)

Figure 3. Chemical structures of (a) poly(*m*-phenylene isophthalate) (Nomex®), (b) poly(*p*-phenylene terephthalamide) (Kevlar®), and (c) polybenzimidazole (PBI®).

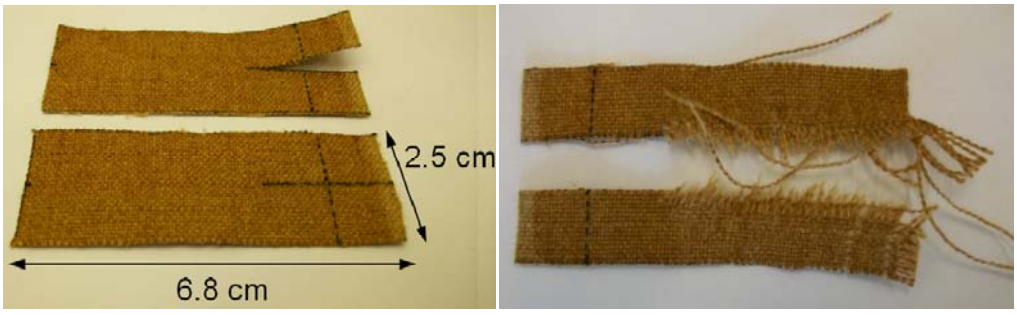

(a) (b)

Figure 4: Fabric swatch (a) before and (b) after tear strength experiment.

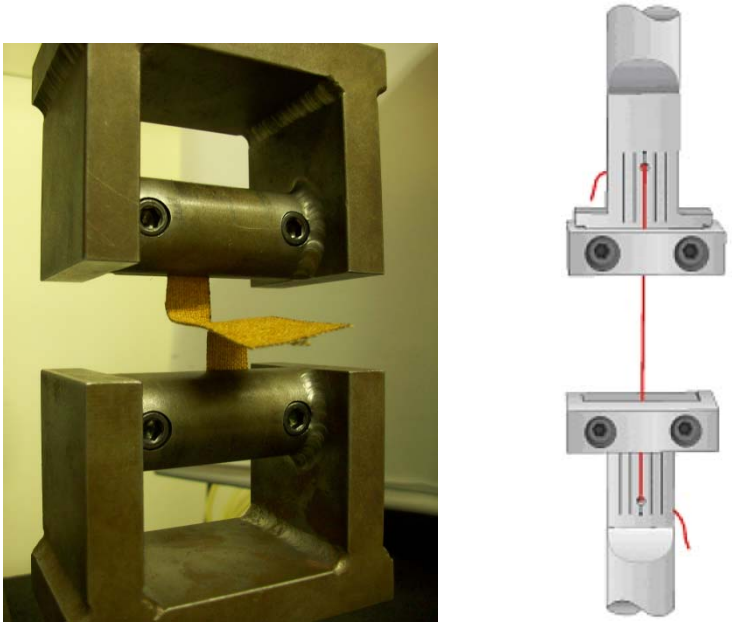

(a) **(b)**

Figure 5: Custom Grips on Instron for tear strength (a) and tensile strength (b) experiments.

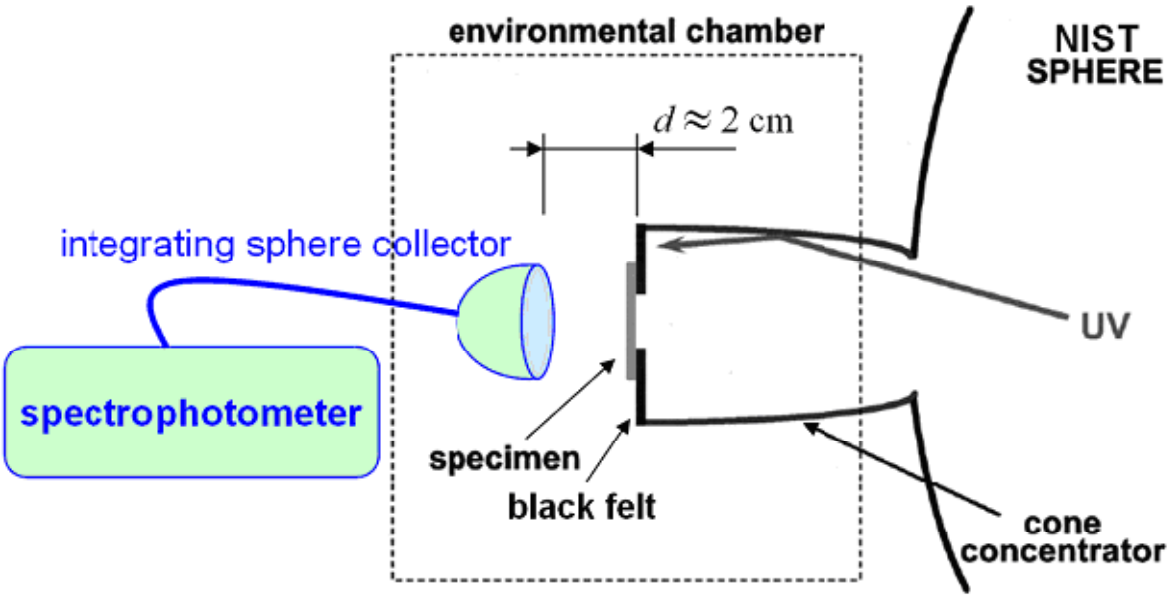

Figure 6: Schematic of UV transmittance measurement.

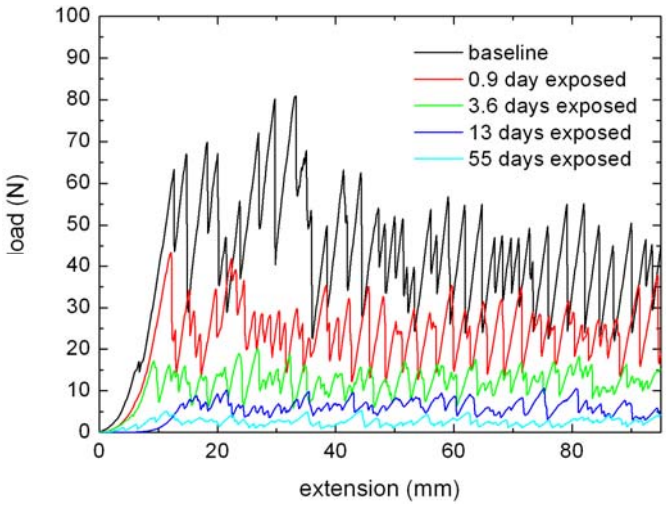

(a)

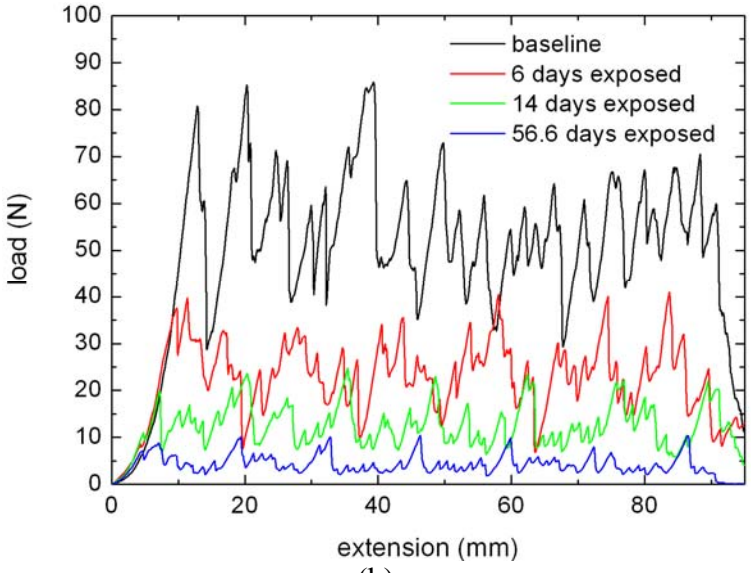

(b)

Figure 7: Representative load-extension curves from tear resistance experiments of (a) NKB and (b) PKB fabrics.

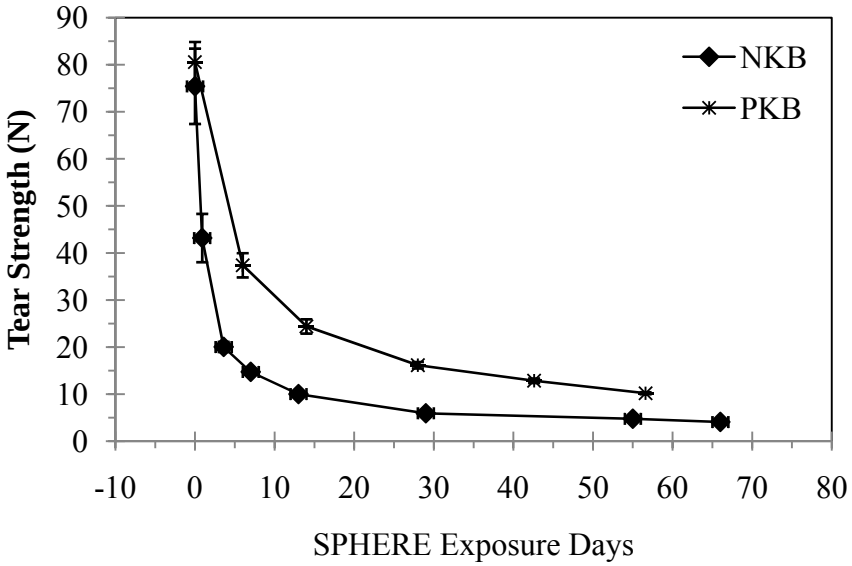

Figure 8: Tear strength of fabrics as a function of SPHERE exposure time at 50 °C and 50% RH. Error bars are ± 1 standard deviation (Tables 2 and 3).

Table 2. Tear strength as a function of UV exposure time at 50 °C and 50% RH for NKB.

SPHERE Exposure Days	Natural Exposure Days	Tear Strength (N)	Tear Strength Decrease
0	0	75.43 ± 8.01	0%
0.9	18	43.18 ± 5.13	43%
3.6	71	20.04 ± 1.08	73%
7.0	139	14.73 ± 0.30	80%
13.0	257	10.01 ± 0.26	87%
29.0	574	5.93 ± 0.65	93%
55.0	1089	4.77 ± 0.56	94%
66.0	1307	4.09 ± 0.12	95%

Table 3. Tear strength as a function of UV exposure time at 50 °C and 50% RH for PKB.

SPHERE Exposure Days	Natural Exposure Days	Tear Strength (N)	Tear Strength Decrease
0	0	80.56 ± 4.30	0%
6	119	37.39 ± 2.58	54%
14	277	24.39 ± 1.52	70%
28	554	16.15 ± 0.69	80%

42.6	843	12.85 ± 0.49	84%
56.6	1121	10.19 ± 0.20	87%

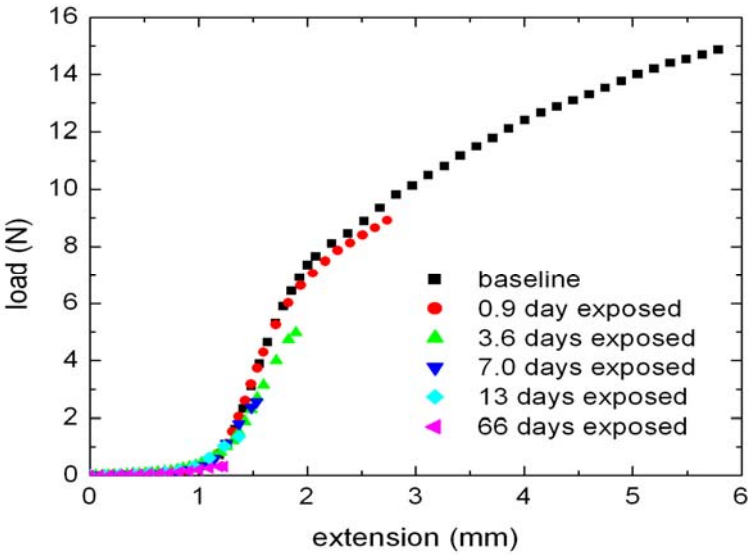

(a)

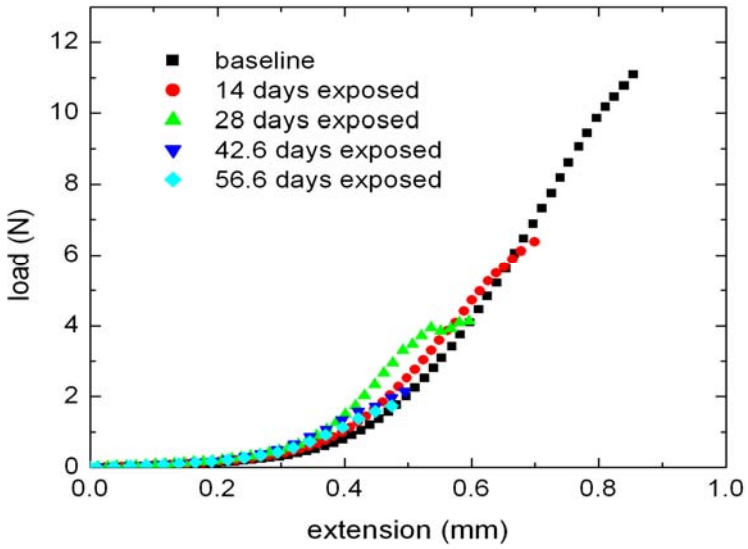

(b)

Figure 9: Representative stress-strain curves from yarn tensile strength experiments of (a) NKB and (b) PKB fabrics.

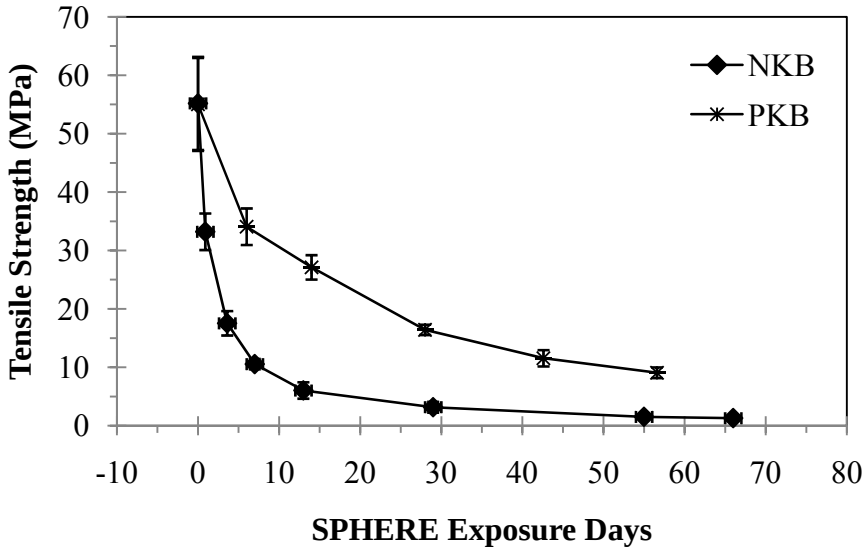

(a)

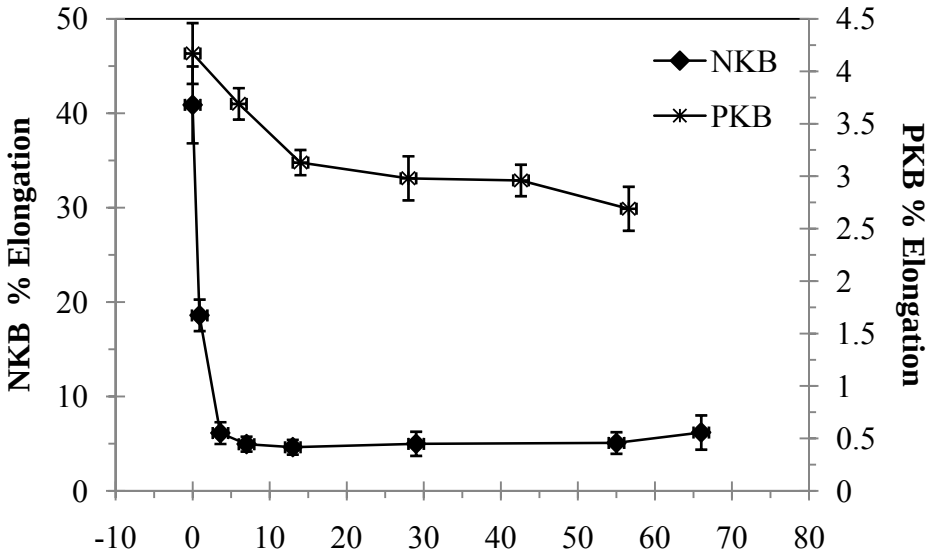

(b)

Figure 10: (a) Tensile strength and (b) % elongation of fabrics as a function of SPHERE exposure time at 50 °C and 50% RH. Error bars are ± 1 standard deviation (Tables 4 and 5).

Table 4. Tensile strength and % elongation as a function of UV exposure time at 50 °C and 50% RH for NKB.

SPHERE Exposure (d)	Natural Exposure (d)	Tensile Strength (MPa)	Tensile Strength Decrease	%-Elongation	%Elongation Decrease
0	0	55.2 ± 7.97	0%	40.89 ± 4.07	0%
0.9	18	33.22 ± 3.13	40%	18.6 ± 1.67	55%

3.6	71	17.55 ± 2.09	68%	6.13 ± 1.15	85%
7.0	139	10.56 ± 0.88	81%	4.96 ± 0.79	88%
13.0	257	6.05 ± 1.4	89%	4.63 ± 0.78	89%
29.0	574	3.18 ± 0.92	94%	4.99 ± 1.28	88%
55.0	1089	1.53 ± 0.43	97%	5.08 ± 1.14	88%
66.0	1307	1.31 ± 0.27	98%	6.19 ± 1.81	85%

Table 5. Tensile strength and % elongation as a function of UV exposure time at 50 °C and 50% RH for PKB.

SPHERE Exposure (d)	Natural Exposure (d)	Tensile Strength (MPa)	Tensile Strength Decrease	% Elongation	% Elongation Decrease
0	0	55.03 ± 5.30	0%	4.17 ± 0.29	0%
6	119	34.08 ± 5.60	38%	3.69 ± 0.28	12%
14	277	27.13 ± 3.22	51%	3.13 ± 0.26	25%
28	554	16.43 ± 2.19	70%	2.98 ± 0.37	29%
42.6	843	11.56 ± 2.41	79%	2.96 ± 0.55	29%
56.6	1121	9.08 ± 1.48	83%	2.69 ± 0.48	35%

Table 6: Ultraviolet protection factor (UPF) and the average UV transmittance of NKB.

Exposure time (days)	UPF	$T_{(280\text{-}400)}$ (%)	$T_{(280\text{-}315)}$ (%)	$T_{(315\text{-}400)}$ (%)	$T_{(400\text{-}500)}$ (%)
0.0	43.35	0.12	0.00	0.17	0.10
13.0	23.86	0.18	0.00	0.26	0.41
29.0	17.74	0.18	0.00	0.26	0.57
55.0	17.73	0.23	0.00	0.33	0.56
66.0	18.34	0.24	0.00	0.34	0.54

Table 7: Ultraviolet protection factor (UPF) and the average UV transmittance of PKB.

Exposure time (days)	UPF	$T_{(280\text{-}400)}$ (%)	$T_{(280\text{-}315)}$ (%)	$T_{(315\text{-}400)}$ (%)	$T_{(400\text{-}500)}$ (%)
0.0	23.83	0.12	0.10	0.12	0.22
14.0	18.21	0.08	0.05	0.10	0.17

28.0	17.05	0.08	0.03	0.11	0.14
42.6	18.21	0.11	0.04	0.14	0.20
56.6	18.95	0.17	0.36	0.09	0.14

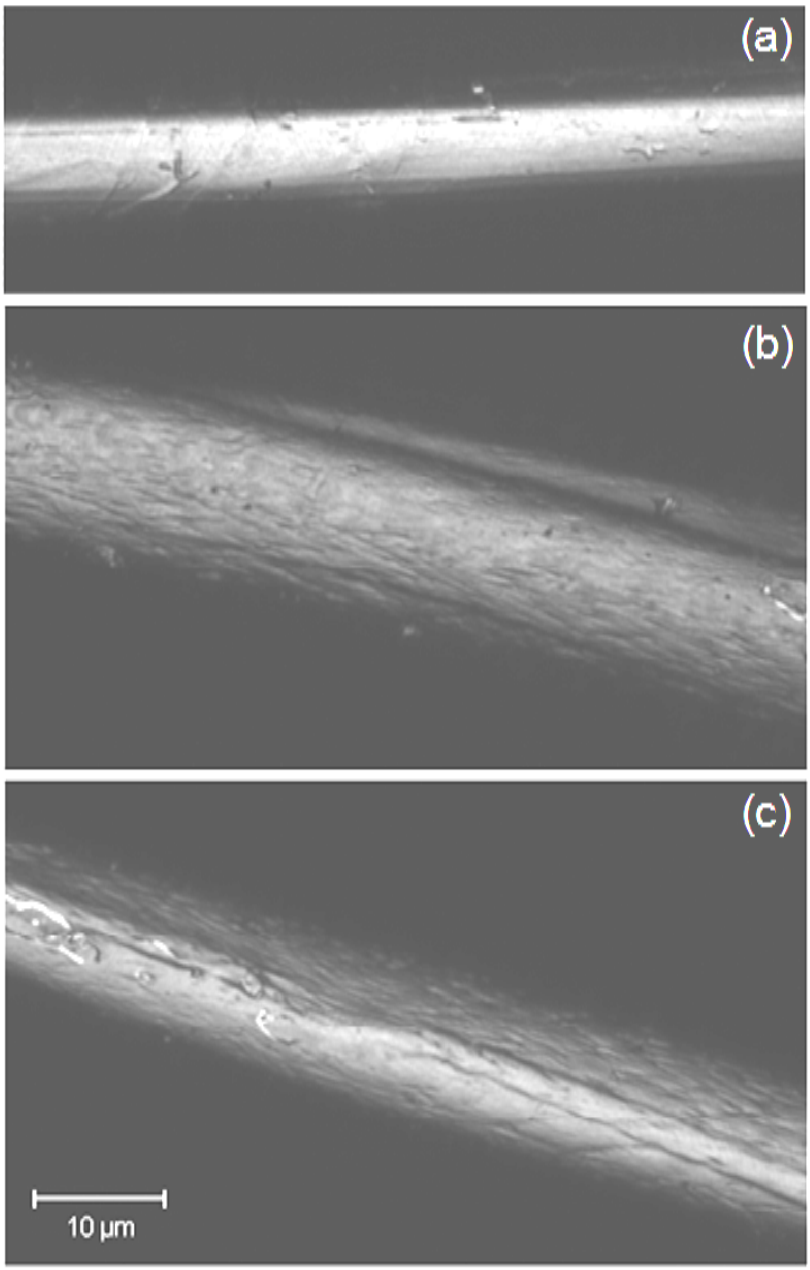

Figure 11: Confocal microscope images of poly(*m*-phenylene isophthalate) fibers from NKB following (a) 0 d, (b) 13 d, and (c) 66 d of UV exposure at 50 °C and 50% RH.

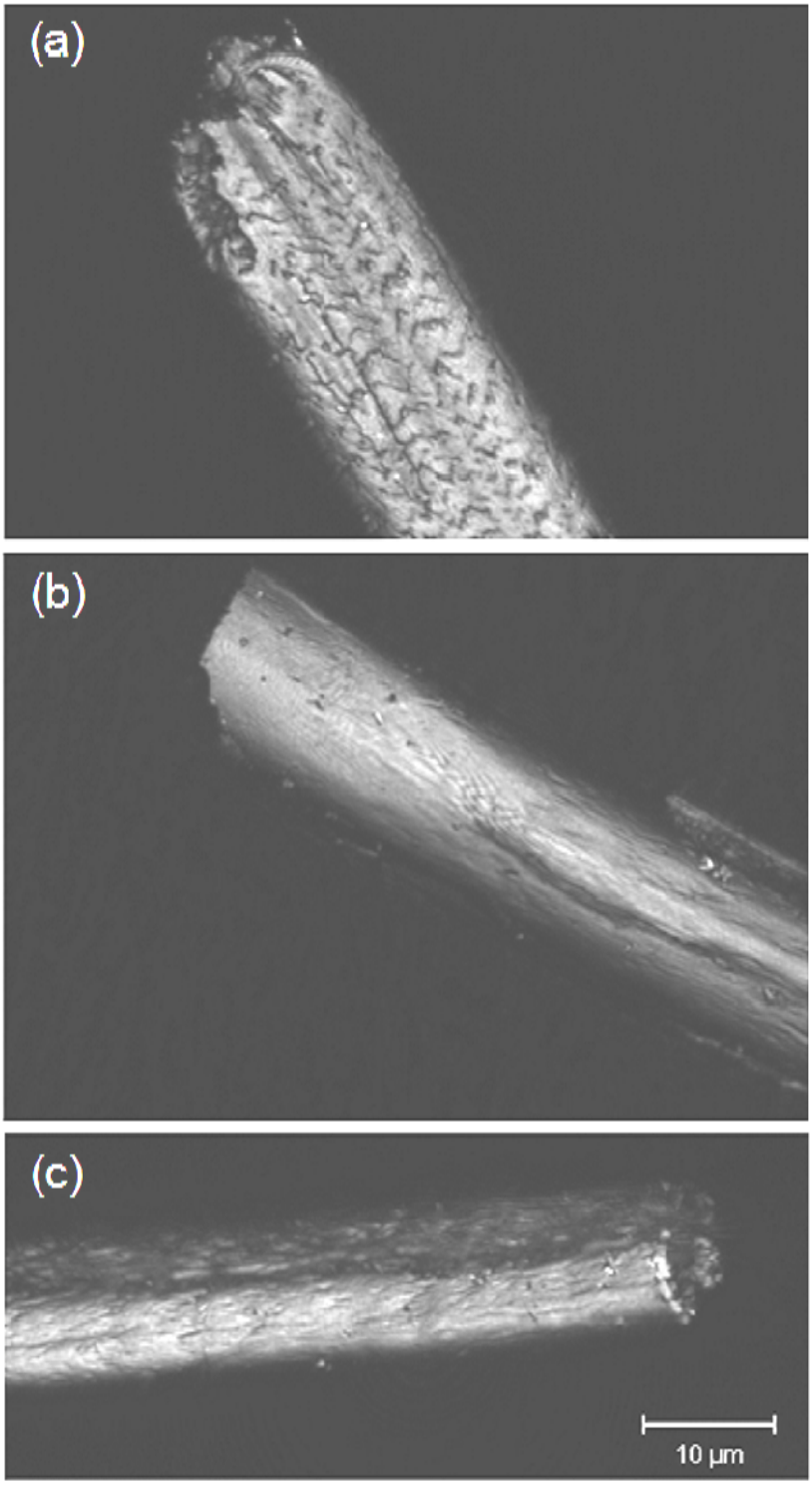

Figure 12: Confocal microscope images of poly(*m*-phenylene isophthalate) fiber fracture ends following tensile failure. These fibers are from NKB fabric following (a) 0 d, (b) 13 d, and (c) 66 d of UV exposure at 50 °C and 50% RH.

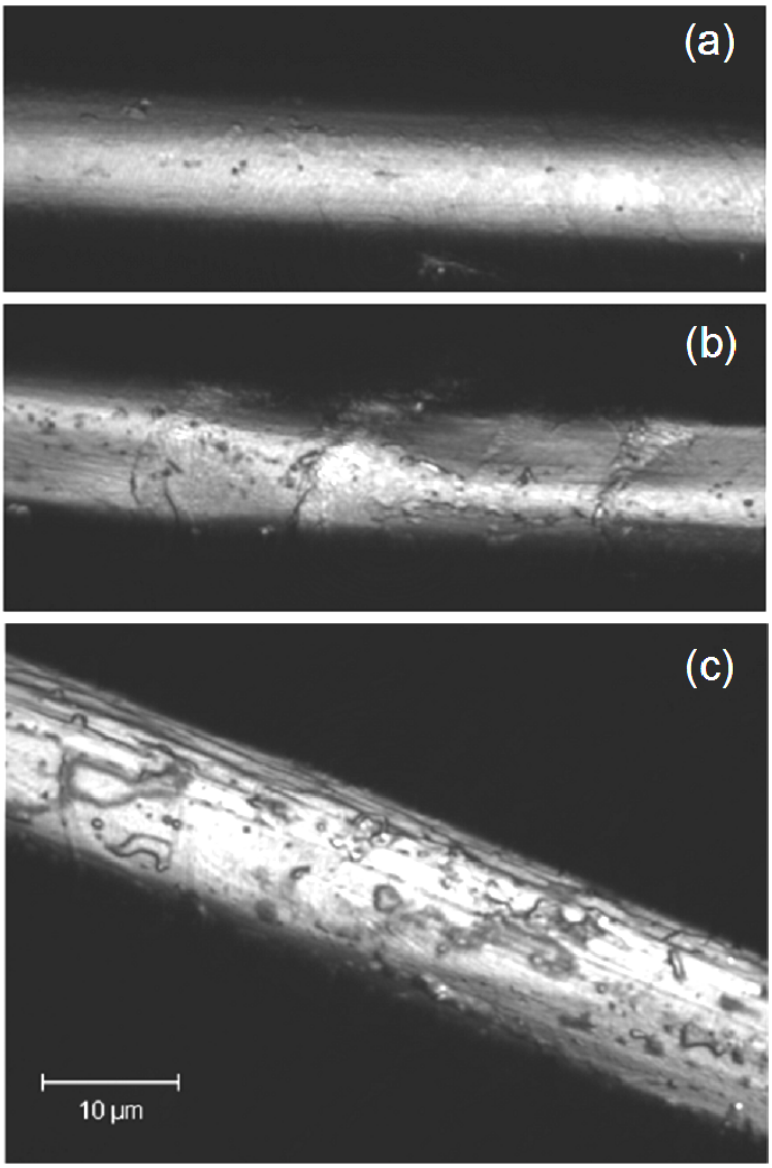

Figure 13: Confocal microscope images of poly(*p*-phenylene terephthalamide) fibers from PKB following (a) 0 d, (b) 14 d, and (c) 56.6 d of UV exposure at 50 °C and 50% RH.

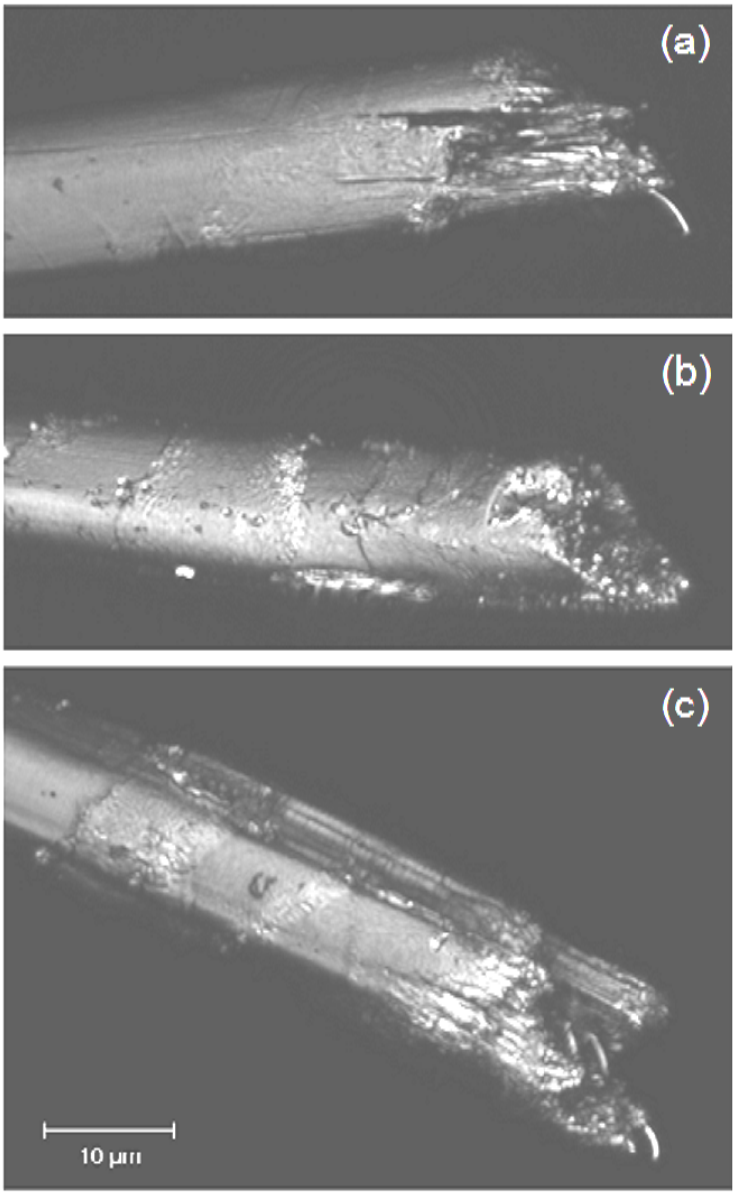

Figure 14: Confocal microscope images of poly(*p*-phenylene terephthalamide) fiber fracture ends following tensile failure. These fibers are from PKB fabric following (a) 0 d, (b) 14 d, and (c) 56.6 d of UV exposure at 50 °C and 50% RH.

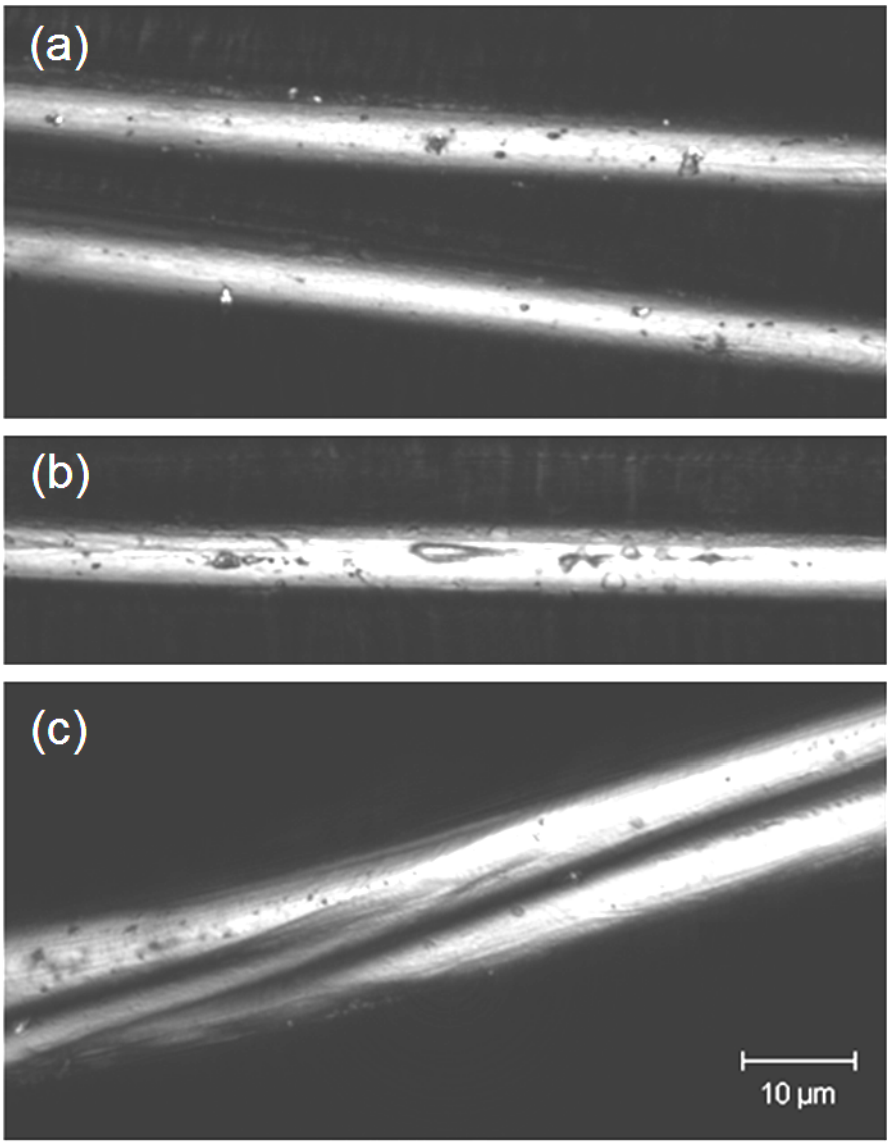

Figure 15: Confocal microscope images of polybenzimidazole fibers from PKB following (a) 0 d, (b) 14 d, and (c) 56.6 d of UV exposure at 50 °C and 50% RH.

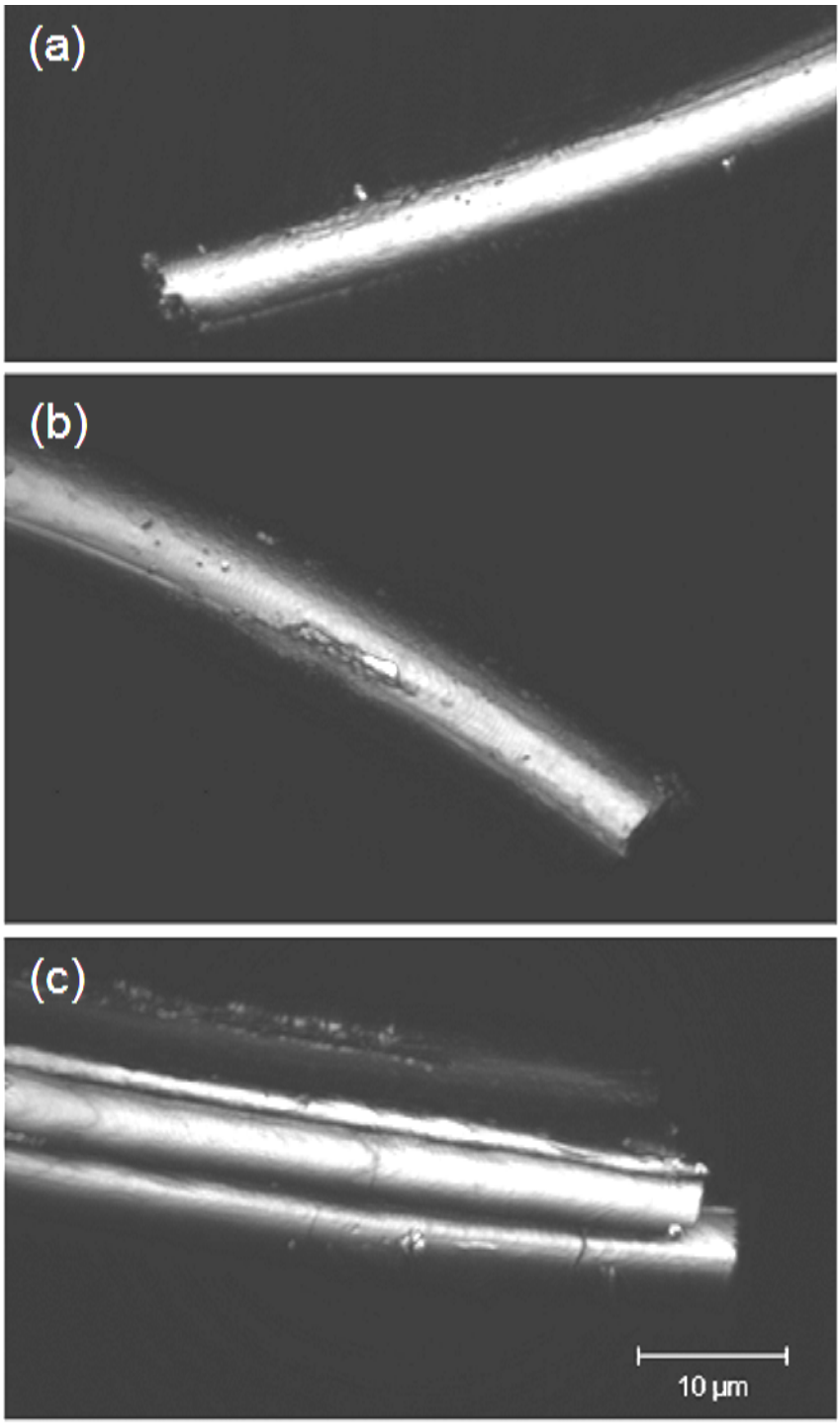

Figure 16: Confocal microscope images of polybenzimidazole fiber fracture ends following tensile failure. These fibers are from PKB fabric following (a) 0 d, (b) 14 d, and (c) 56.6 d of UV exposure at 50 °C and 50% RH.

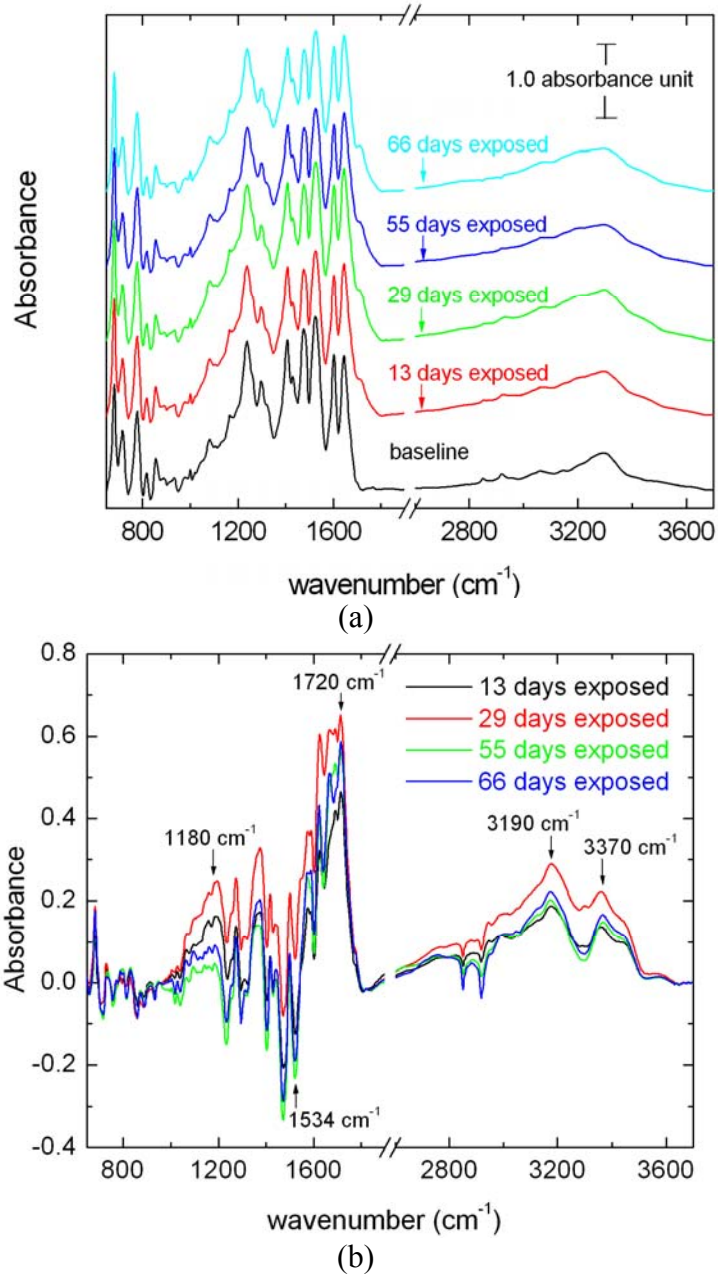

Figure 17: (a) ATR-FTIR spectra of unexposed and exposed NKB and (b) the difference spectra.

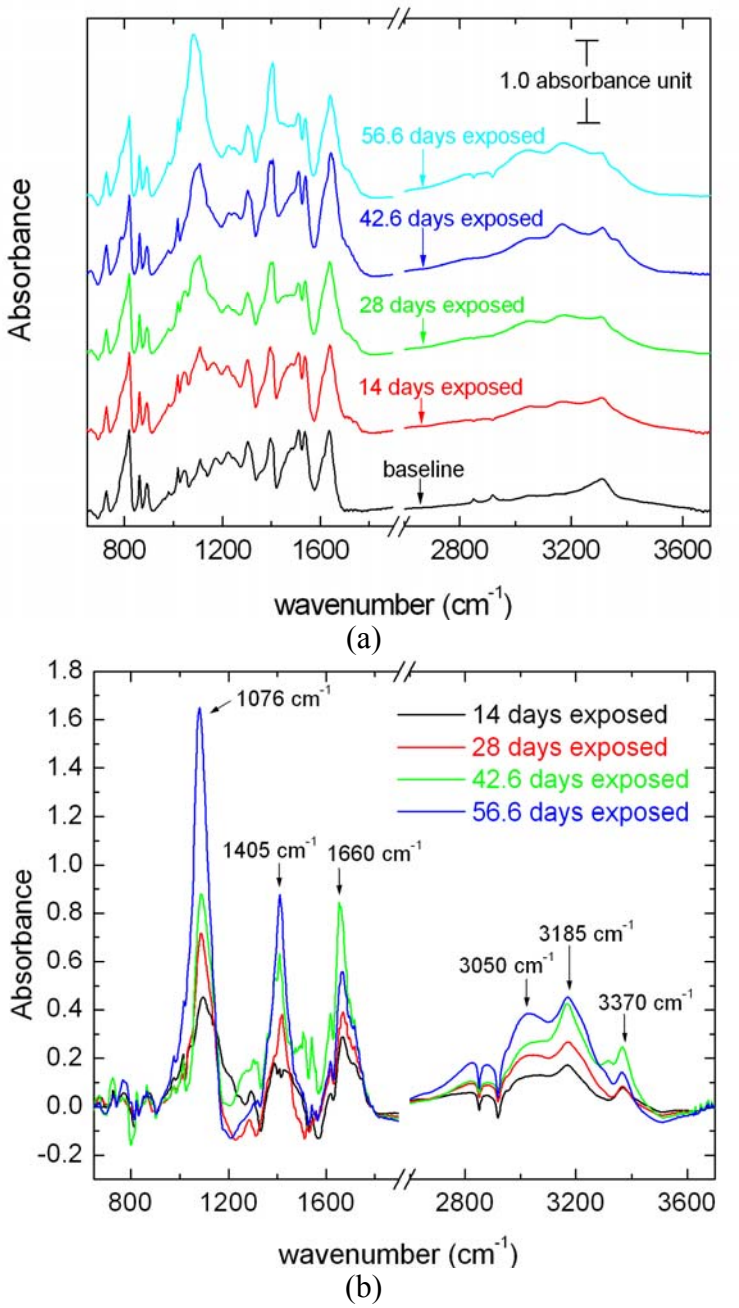

Figure 18: (a) ATR-FTIR spectra of unexposed and exposed PKB and (b) the difference spectra.

References

[1] Picture provided by SPERIAN Protective Apparel, Ltd.

[2] H. Zhang, J. Zhang, J. Chen, X. Hao, S. Wang, X. Feng, Y. Guo, Effects of solar irradiation on the tensile properties and structure of PPTA, *Polym. Degrad. Stab.*, **Vol. 91**, 2761, 2006.

[3] J. Chin, A. Forster, C. Clerici, L. Sung M. Oudia, K. Rice, Temperature and humidity aging of poly(p-peylene-2,6-benzobisoazole) fibers: Chemical and physical characterization, *Polym Degrad. Stab.*, **Vol. 92**, 1234, 2007.

[4] W.C. Tincher, W.C. Carter, D.R. Gentry, Protection of Nomex® from Ultraviolet Degradation, *Technical Report ASD-TR-7711 from Georgia Tech to Air Force,* Accession Number ADA041494, March 1977.

[5] NFPA 1971, *Standard on Protective Ensembles for Structural Fire Fighting and Proximity Fire Fighting 2007 edition.*

[6] NFPA 1851, *Standard on Selection, Care, and Maintenance of Protective Ensembles for Structural Fire Fighting and Proximity Fire Fighting 2008 edition*.

[7] Kombat™ and Defender™ are registered trademarks of TenCate™ SouthernMills™, http://www.tencate.com/smartsite.dws?lang=en&id=3792, last viewed on 10/26/09.

[8] Shelltite™ and Super Shelltite™ are registered trademarks of TenCate™ SouthernMills™.

[9] PBI Performance Incorporated, http://www.pbigold.com/, last viewed on 10/26/09.

[10] Nomex® and Kevlar® are registered trademarks of the DuPont™ Corporation.

[11] J. Chin, E. Byrd, N. Embree, J. Garver, B. Dickens, T. Finn, and J. Martin, *Review of Scientific Instruments*, **Vol.75**, 4951, 2005.

[12] Standard Test Method for Tearing Strength of Fabrics by the Tongue (Single Rip) Procedure (Constant-Rate-of-Extension Tensile Testing Machine), *ASTM D 2261-96*, 2002.

[13] B. Dickens, J.W. Martin, and D.R. Bauer, Service Life Prediction Methodology and Metrologies, *American Chemical Society*, 2001.

[14] Transmittance or Blocking of Erythemally Weighted Ultraviolet Radiation through Fabrics, *AATCC Test Method 183-2000*, 2004.

[15] M. Gorenšek and F. Sluga, *Textile Res. J.*, **Vol. 74**, 469, 2004.

[16] C.R. Roy and H.P. Gies, *Radiation Protection Dosimetry*, **Vol. 72**, 231, 1997.

[17] H.E. Nasr, S.M. Sayyah, D.M. Essa, S.H. Samaha, and A.M. Rabie, *Carbohydrate Polymers*, **Vol. 76**, 36, 2009.

[18] J. W. S. Hearle, B. Lomas, William D. Cooke, *Atlas of fiber fracture and damage to textiles*, 2nd edition, Textile Institute, CRC, Manchester, England, 1998.

[19] S. Villar-Rodil, J.I. Paredes, A. Martine-Alonso, and J.M.D. Tascón, *Chem. Mater.*, **Vol. 13**, 4297, 2001.

[20] Z. Chang, H. Pu, D. Wan, L. Liu, J. Yuan, and Z. Yang, *Polym. Degrad. Stab.*, **Vol. 94**, 1206, 2009.

[21] M. Y. Jang, and Y Yamazaki, *Solid State Ionics*, **Vol.167**, 107, 2004.

[22] John Coates, "Encyclopedia of Analytical Chemistry", *John Wiley & Sons*, Chichester, 2000.

[23] A.M. Tiefenthaler, and M.W. Urban, *Appl. Spectro.*, **Vol. 42**, 163, 1988.
[24] V. Deimede, G. A. Voyiatzis, J.K. Kallitsis, L. Qingfeng, and N.J. Bjerrum, *Macromolecules*, **Vol. 33**, 7609, 2000.